Crystal Structure and Magnetic Properties of the Novel Hollandite $Ba_{1.3}Co_{1.3}Ti_{6.7}O_{16}$

Larysa Shlyk and Rainer Niewa

Institut für Anorganische Chemie, Universität Stuttgart, Pfaffenwaldring 55, 70569 Stuttgart, Germany

Reprint requests to Prof. Dr. Rainer Niewa. Fax: +49(0)71-685-64241.
E-mail: rainer.niewa@iac.uni-stuttgart.de

Z. Naturforsch. **2011**, *66b,* 1097 – 1100; received September 20, 2011

Single crystals of the new barium hollandite $Ba_{1.3}Co_{1.3}Ti_{6.7}O_{16}$ were obtained from a $BaCl_2$ flux ($I2/m$, $Z = 1$, $a = 9.9470(4)$, $b = 2.9714(2)$, $c = 10.2260(5)$ Å, $\beta = 90.906(2)^\circ$). In the crystal structure piles of Ba atoms are situated within a framework of edge- and vertex-sharing octahedra $(Co,Ti)O_6$. The composition was deduced from microprobe analyses, structure refinements and charge balance arguments in agreement with the observed magnetic properties. The temperature dependence of the magnetic susceptibility $\chi(T)$ of $Ba_{1.3}Co_{1.3}Ti_{6.7}O_{16}$ single crystals reveals paramagnetism down to 2 K. The value of the Co magnetic moment deduced from the Curie-Weiss law agrees well with the theoretical value of the high-spin state spin-only moment of $\mu_{eff} = 3.87\ \mu_B$ for Co^{2+} ($S = 3/2$).

Key words: Hollandite, Cobaltate, Titanate

Introduction

The crystal structure of hollandite was first studied by Bystrom and Bystrom in 1949 [1], based on the earlier results obtained by Cole, Wadsley and Walkley (1947) [2]. Hollandites are characterized by frameworks of egde- and vertex-sharing octahedra forming one-dimensional tunnel structures which host larger cations. The general formula can be written according to $A_xM_8O_{16}$ with typically $x \geq 1$, A = alkali metal, alkaline-earth metal or Pb^{2+}, and M being a wide variety of cations with positive charges of 1, 2, 3, 4, or rarely 5. Although hollandites have been extensively studied due to potential applications, for example as solid-state electrolytes, electrode materials and catalysts, little attention has been paid to their magnetic properties [3 – 5].

The quasi-one-dimensional structure of hollandites demonstrates a broad spectrum of complex quantum-mechanical phenomena at low temperatures, including one-dimensional electron conductivity in KRu_4O_8, $RbRu_4O_8$, and $Cs_{0.8}Li_{0.2}Ru_4O_8$ [6, 7], a quantum phase transition in $BaRu_6O_{12}$ [8], a metal-insulator transition in $K_2V_6O_{16}$ [9 – 12] and $Bi_xV_8O_{16}$ [13, 14], the appearance of ferromagnetism in the diluted semiconductor $K_xTi_8O_{16}$ [15], phase transitions in $K_2Cr_8O_{16}$ from a paramagnet to a metallic ferromagnet and then to an insulating ferromagnet as the temperature is lowered [16].

From a technological point of view, some Ba- or Sr-based Ti-bearing hollandites were reported to have promising dielectric properties for use in microwave devices [17]. Furthermore, the use of barium hollandites in the field of nuclear waste immobilization for the safe storage of radioactive Cs-135 and Cs-137 in the synthetic mineral assemblage has to be pointed out (SYNROC) [18, 19]. The barium hollandites are particularly important since Cs can be substituted for Ba without any substantial change in the resistance to chemical attack. In the area of high-level radioactive waste the Ti-bearing hollandites [18, 20 – 22], *e. g.*, $Ba_{1.2}Mg_{1.2}Ti_{6.8}O_{16}$, have been selected as hosts. A use of Ti is indispensable in order to compensate the charge imbalance as a result of the Cs decay.

The pure titanium hollandite $Ba_xTi_8O_{16}$ retains electroneutrality due to the presence of Ti^{3+} next to Ti^{4+}, *i. e.*, $Ba_x(Ti^{3+})_{2x}(Ti^{4+})_{8-2x}O_{16}$ [23]. A second possibility to reach electroneutrality in Ti-based hollandites is the substitution of some Ti by a metal ion with a charge lower than +4. If sufficient amounts of M^{3+} or M^{2+} are provided, Ti may exclusively stay in the valence state +4. We have realize this situation in the title compound $Ba_xCo_xTi_{8-x}O_{16}$ with $x = 1.28(1)$.

Results and Discussion

Crystal structure and composition

Chemical μ-probe analyses of hollandite crystals, including the very crystal used for structure determination, result in $n(\mathrm{Ba})/n(\mathrm{Co})/n(\mathrm{Ti}) = 1.4 \pm 0.7 : 1.3 \pm 0.2 : 6.7 \pm 0.2$. In the structure refinements based on X-ray diffraction intensity data (Tables 1 – 4) we were unable to discriminate between Co and Ti due to the small difference in the number of electrons coupled with the apparent mixed occupation of crystallographic sites. Therefore, in the refinements the presence of equimolar amounts of Co and Ba was assumed, leading to the composition $Ba_{1.28(1)}Co_{1.28}Ti_{6.72}O_{16}$, in good agreement with results from the μ-probe. Charge balance is possible with the presence of exclusively Co^{2+} next to Ti^{4+}, which agrees with the results from the analysis of the magnetic properties (see below).

In the well known hollandite-type crystal structure of $Ba_{1.3}Co_{1.3}Ti_{6.7}O_{16}$ double-chains of edge-sharing $(Co,Ti)O_6$ octahedra run along [010] and are further interconnected *via* vertices within (010) to form a three-dimensional framework with one-dimensional channels along [010]. Fig. 1 shows a section of the crystal structure viewed in this crystallographic direction. Ba is situated within the larger one-dimensional channels. Tetragonal and monoclinic hollandites are well known in the literature. The distortion from tetragonal to monoclinic typically occurs when the channels in the host framework are too large for the guest atoms. For $Ba_{1.3}Co_{1.3}Ti_{6.7}O_{16}$ we observe the monoclinic structure variant. Although for examples of both tetragonal and monoclinic variants incommensurately modulated structure refinements were presented [*e. g.*, 24 – 27], from our single-crystal X-ray diffraction data we have no indications for a modulation. The common structure model with a simple three-dimensional commensurate description results in a Ba position with an occupancy below 1 and short distances within the resulting Ba chain of 0.832(2) and 2.139(2) Å. The maximum physically possible occupancy would be 50 %

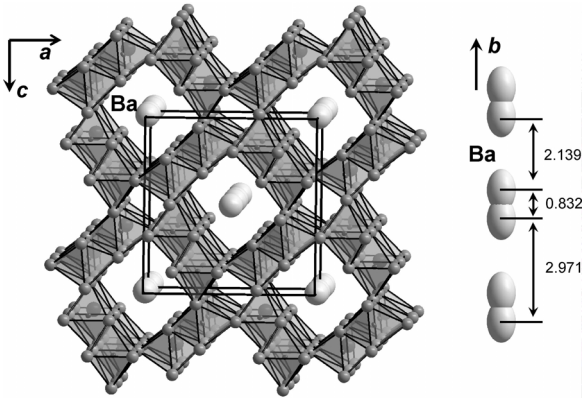

Fig. 1. Left: View of the crystal structure of the hollandite $Ba_{1.3}Co_{1.3}Ti_{6.7}O_{16}$ along [010]. The framework of edge- and vertex-sharing oxometalate octahedra hosts Ba ions. Right: Arrangement of Ba positions along a pile in [001]. Positions in the commensurate structure description are occupied statistically by 32 %.

Table 1. Selected crystal structure, data collection and refinement parameters for $Ba_{1.28(1)}Co_{1.28}Ti_{6.72}O_{16}$.

Crystal system	monoclinic
Space group	$I2/m$
a, Å	9.9470(4)
b, Å	2.9714(2)
c, Å	10.2260(5)
β, deg	90.906(2)
Z	1
Density (calcd.), g cm^{-3}	4.56
Volume, Å^3	302.21
Diffractometer	Nonius-κ-CCD
Radiation; wavelength, Å	MoK_α; λ = 0.7107
Index ranges hkl	± 13, ± 3, ± 13
θ_{max}, deg	28.16
$F(000)$, e	382.1
μ(MoK_α), mm^{-1}	10.1
Reflections collected / independent	3259 / 438
Data averaging: R_{int} / R_σ	0.0672 / 0.0307
R_1 ($\lvert F_o\rvert \geq 4\sigma(F_o)$)	0.0289
R_1 / wR_2 / *GooF* (all data)	0.0325 / 0.0800 /1 .212
Largest e$^-$ diff. peak / hole, Å^{-3}	0.81 / −0.93

Table 2. Atomic coordinates and isotropic displacement parameters (Å^2) for $Ba_{1.28(1)}Co_{1.28}Ti_{6.72}O_{16}$.

Atom	Site	x/a	y/b	z/c	U_{iso}
Ba[a]	4*g*	0	0.3600(4)	0	0.0218(4)
M(1)[b]	4*i*	0.34842(7)	0	0.16462(7)	0.0088(3)
M(2)[b]	4*i*	0.83160(7)	0	0.35298(7)	0.0087(3)
O(1)	4*i*	0.1961(3)	0	0.8426(3)	0.0080(6)
O(2)	4*i*	0.1501(3)	0	0.2035(3)	0.0091(6)
O(3)	4*i*	0.1769(3)	0	0.4595(3)	0.0099(6)
O(4)	4*i*	0.4596(3)	0	0.8432(3)	0.0090(6)

[a] Occupied by 0.319(2) Ba; [b] fixed occupation with 84 % Ti, 16 % Co.

Table 3. Anisotropic displacement parameters (Å^2) for $Ba_{1.28(1)}Co_{1.28}Ti_{6.72}O_{16}$ ($U_{12} = U_{23} = 0$ for all sites).

Atom	U_{11}	U_{22}	U_{33}	U_{13}
Ba(1)	0.0156(5)	0.0327(7)	0.0171(5)	0.0011(3)
M(1)	0.0095(4)	0.0057(5)	0.0114(4)	0.0042(3)
M(2)	0.0116(4)	0.0052(5)	0.0094(4)	−0.0013(3)
O(1)	0.008(1)	0.008(2)	0.008(1)	0.002(1)
O(2)	0.008(1)	0.008(2)	0.011(1)	0.001(1)
O(3)	0.013(1)	0.011(2)	0.006(1)	0.002(1)
O(4)	0.008(1)	0.008(2)	0.011(1)	0.003(1)

Table 4. Selected interatomic distances (Å) for $Ba_{1.28(1)}Co_{1.28}Ti_{6.72}O_{16}$.

Ba	–Ba	0.832(2)	1×	*M*(1)	–O(4)	1.912(3)	1×
	–Ba	2.139(2)	1×		–O(3)	1.968(2)	2×
	–Ba	2.9714(2)	2×		–O(2)	2.007(2)	2×
	–O(2)	2.758(3)	2×		–O(2)	2.019(3)	1×
	–O(1)	2.764(3)	2×	*M*(2)	–O(3)	1.920(3)	1×
	–O(2)	3.174(2)	2×		–O(4)	1.961(2)	2×
	–O(1)	3.180(2)	2×		–O(1)	2.008(2)	2×
	–O(3)	3.261(2)	2×		–O(1)	2.014(3)	1×
	–O(4)	3.563(2)	2×				

and for our unit cell results in shortest distances *d*(Ba–Ba) = 2.9714(2) Å along this chain in an ordered model (compare Fig. 1). However, the refinements converge at an occupancy of 31.9(2) %. Selected interatomic distances, which all lie in the expected ranges, are summarized in Table 4.

Magnetic properties

Fig. 2 shows data for the magnetic susceptibility $\chi = M/H$ for several $Ba_{1.3}Co_{1.3}Ti_{6.7}O_{16}$ single crystals allowing free rotation in an applied field of μH = 0.05 T. $Ba_{1.3}Co_{1.3}Ti_{6.7}O_{16}$ single crystals show typical paramagnetic behavior with a lack of any long-range magnetic order down to 2 K. The inverse magnetic susceptibility $1/\chi$, plotted in the inset of Fig. 2, shows no significant deviation from linearity down to 2 K. Above 50 K the susceptibility data follow the Curie-Weiss law $\chi = C/(T - \Theta_W)$ with a low Weiss temperature Θ_W = 6.4 K, indicating that the Co ions in the sample are very weakly coupled by ferromagnetic exchange. The value of μ_{eff} is calculated from $C = N_A\mu_{eff}{}^2\mu_B/3k_B$ (where N_A is the Avogadro number, μ_B is the Bohr magneton, k_B is the Boltzmann constant, and μ_{eff} is the effective magnetic moment). The effective magnetic moment deduced from the Curie-Weiss fitting is, therefore, μ_{eff} = 3.62 μ_B. This value is in good agreement with that expected for the high-spin state spin-only moment of μ_{eff} = 3.87 μ_B for Co^{2+} (S = 3/2). Moreover, the divalent state of Co in this material is supported by charge balance considerations. The electrical resistance of the single crystal $Ba_{1.3}Co_{1.3}Ti_{6.7}O_{16}$ at r. t. is $R_{300\,K} \sim 100\ M\Omega$, which is very high, and in the range of typical insulators.

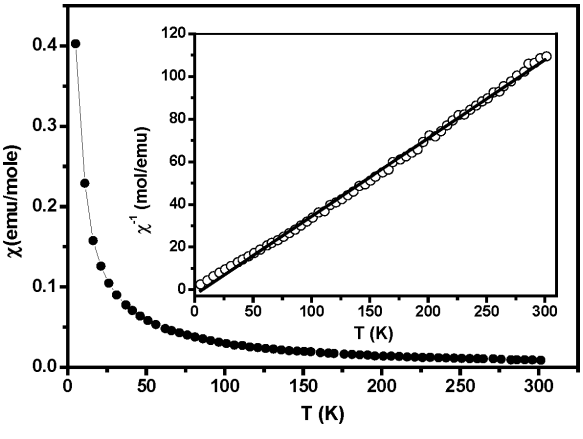

Fig. 2. Temperature dependence of the field-cooled DC magnetic susceptibility $\chi(T)$ of $Ba_{1.3}Co_{1.3}Ti_{6.7}O_{16}$ single crystals in an applied magnetic field $\mu_o H$ = 0.05 T. The inset shows the inverse magnetic susceptibility *vs.* temperature. The solid line is a fit of the data to the Curie-Weiss law.

Experimental Section

For single-crystal growth of $Ba_{1.3}Co_{1.3}Ti_{6.7}O_{16}$, initial amounts of 6.2 mmol TiO_2, 1.7 mmol Co_3O_4 and 3.2 mmol $BaCl_2$ were mixed and then pressed into a pellet. The pellet was heated to 1350 °C and kept at this temperature for several days. Then the furnace was slowly allowed to cool to r. t. Green crystals with maximum sizes of 0.5 mm^3 were mechanically extracted from the product.

Single-crystal X-ray diffraction data collection was performed using a 4 circle diffractometer (NONIUS-κ-CCD, Bruker AXS GmbH) with monochromatic MoK_α radiation. Selected information concerning the data collection and structure refinements is summarized in Tables 1 – 4.

Further details of the crystal structure investigations may be obtained from Fachinformationszentrum Karlsruhe, 76344 Eggenstein-Leopoldshafen, Germany (fax: +49-7247-808-666; e-mail: crysdata@fiz-karlsruhe.de, http://www.fiz-informationsdienste.de/en/DB/icsd/depot_anforderung.html) on quoting the deposition number CSD-423585.

Chemical μ-probe analyses result in very consistent compositions observed for all crystals investigated with the average atomic density ratios n(Ba)/n(Co)/n(Ti) = $1.4 \pm 0.7 : 1.3 \pm 0.2 : 6.7 \pm 0.2$ (the oxygen content could not be quantified with this technique). No additional elements were detected.

The magnetization data for free to rotate single crystals were acquired over a temperature range 2 K $\leq T \leq$ 300 *K* in applied magnetic fields $0 \leq \mu_o H \leq 5$ T using a Quantum Design MPMS7 magnetometer.

Acknowledgements

We would like to thank Dr. F. Lissner for collecting the X-ray diffraction data and K. Wolff for the EDX measurements. Additionally, we gratefully acknowledge the use of a SQUID magnetometer located in the group of Prof. M. Dressel.

[1] A. Bystrom, A. M. Bystrom, *Acta Crystallogr.* **1950**, **3**, 146 – 154; *ibid.* **1951**, **4**, 469.
[2] W. F. Cole, A. D. Wadsley, A. Walkley, *Trans. Electrochem. Soc.* **1947**, *92*, 133 – 158.
[3] S. L. Brock, N. G. Duan, Z. R. Tian, O. Giraldo, H. Zhou, S. L. Suib, *Chem. Mater.* **1998**, *10*, 2619 – 2628.
[4] Q. Feng, T. Horiuchi, T. Mitsusio, K. Yanagisawa, N. Yamasaki, *J. Mater. Sci. Lett*. **1999**, *18*, 1375 – 1378.
[5] S. Barbato, J. L. Gautier, *Electrochim. Acta* **2001**, *46*, 2767 – 2776.
[6] W. Kobayashi, *Phys. Rev. B* **2009**, *79*, 155116.
[7] M. L. Foo, W. L. Lee, T. Siegrist, G. Lawes, A. P. Ramirez, N. P. Ong, R. J. Cava, *Mater. Res. Bull.* **2004**, *39*, 1663 – 1670.
[8] Z. Q. Mao, T. He, M. M. Rosario, K. D. Nelson, D. Okuno, B. Ueland, I. G. Deac, P. Schiffer, Y. Liu, R. J. Cava, *Phys. Rev. Lett.* **2003**, *90*, 186601.
[9] A. Maignan, O. I. Lebedev, G. Van Tendeloo, C. Martin, S. Hebert, *Phys. Rev. B* **2010**, *82*, 035122.
[10] Y. Shimizu, K. Okai, M. Itoh, M. Isobe, J. Yamaura, T. Yamauchi, Y. Ueda, *Phys. Rev. B* **2011**, *83*, 155111.
[11] Y. Ishige, T. Sudayama, Y. Wakisaka, T. Mizokawa, H. Wadati, G. A. Sawatzky, T. Z. Regier, M. Isobe, Y. Ueda, *Phys. Rev. B* **2011**, *83*, 125112.
[12] S. Horiuchi, T. Shirakawa, Y. Ohta, *Phys. Rev. B* **2008**, *77*, 155120.
[13] T. Waki, H. Kato, M. Kato, K. Yoshimura, *J. Phys. Soc. Jpn.* **2004**, *73*, 275 – 279.
[14] Y. Shibata, Y. Ohta, *J. Phys. Soc. Jpn.* **2002**, *71*, 513 – 518.
[15] K. Noami, Y. Muraoka, T. Wakita, M. Hirai, Y. Kato, T. Muro, Y. Tamenori, T. Yokoya, *J. Appl. Phys.* **2010**, *107*, 073910.
[16] M. Isobe, S. Koishi, S. Yamazaki, J. Yamaura, H. Gotou, T. Yagi, Y. Ueda, *J. Phys. Soc. Jpn.* **2009**, *78*, 114713.
[17] V. M. Manisha, K. P. Murali, S. N. Potty, V. Priyadarsini, R. Ratheesh, *Bull. Mater. Sci.* **2004**, *27*, 149 – 153.
[18] R. W. Cheary, J. Kwiatkowska, *J. Nucl. Mater.* **1984**, *125*, 236 – 243.
[19] M. L. Carter, E. R. Vance, D. R. G. Mitchell, J. V. Hanna, Z. Zhang, E. Loi, *J. Mater. Res.* **2002**, *17*, 2578 – 2589.
[20] R. W. Cheary, *Acta Crystallogr.* **1987**, *B43*, 28 – 34.
[21] R. W. Cheary, R. Squadrito, *Acta Crystallogr.* **1989**, *B45*, 205 – 212.
[22] R. W. Cheary, *Acta Crystallogr.* **1991**, *B47*, 325 – 333.
[23] R. W. Cheary, *Acta Crystallogr.* **1990**, *B46*, 599 – 609.
[24] X. Shi-Bin, F. Hai-Fu, W. Xiao-Jing, L. Fang-Hua, *Acta Crystallogr.* **1990**, *A46*, 929 – 934.
[25] H. Leligny, Ph. Labbé, M. Ledésert, B. Raveau, C. Valdez, W. H. McCarrol, *Acta Crystallogr.* **1992**, *B48*, 134 – 144.
[26] V. Aubin-Chevaldonnet, P. Deniard, M. Evain, A. Y. Leinekugel-Le-Cocq-Errien, S. Jobic, D. Caurant, V. Petricek, T. Advocat, *Z. Kristallogr*. **2007**, *222*, 383 – 390.
[27] T. Klimczuk, W.-L. Lee, H. W. Zandbergen, R. J. Cava, *Mater. Res. Bull.* **2004**, *39*, 1671 – 1677.